Advanced Materials Research Vol. 936 (2014) pp 295-299
Online available since 2014/Jun/30 at www.scientific.net
© (2014) Trans Tech Publications, Switzerland
doi:10.4028/www.scientific.net/AMR.936.295

A Facile Method to Preparation of Amphiphilic Perylene Tetracarboxylic Diimide/ZnS Hybrid Nanocomposites and Improved Semiconducting Property

Jingang Song[1,a], Hongyan Wang[1,b], Nianshuai An[1,c], Yanli Chen*[1,d]

[1]Shandong Provincial Key Laboratory of Fluorine Chemistry and Chemical Materials, School of Chemistry and Chemical Engineering, University of Jinan, Jinan 250022, China

[a]songjingang1987@126.com, [b]chm_wanghy@ujn.edu.cn, [c]annianshuai@163.com, [d]chm_chenyl@ujn.edu.cn

Keywords: HH-PDI, ZnS, nanocomposite, semiconducting property.

Abstract: A self-assembled film of an amphiphilic perylene tetracarboxylic diimide derivative (N-hexane-N'-(1-phenyl-4-aminoethanol)-1,7-di(4-tert-butylphenoxy)perylene-3,4;9,10-tetracarboxylate diimide, HH-PDI) has been used as the organic template to produce the first example of monodispersed nano-particles of HH-PDI/ZnS composites. The HH-PDI pure film and HH-PDI/ZnS nanocomposites were characterized by UV-vis absorption, X-ray diffraction (XRD), scanning electron microscopy (SEM) and current-voltage (I-V) measurements. Experimental results revealed the film crystallinity and general molecular order for HH-PDI molecules in the nanocomposites are improved effectively in comparison with those in the pure film due to the introduction of ZnS nanocrystals. The electrical conductivity of the HH-PDI/ZnS nanocomposites (6.6×10^{-5} S cm^{-1}) is more than ca. 2 order of magnitude higher than that of (3.6×10^{-7} S cm^{-1}). The present result provides an efficient way to improve the performance of organic semiconductors through introducing inorganic semiconducting nanocrystals.

Introduction

Semiconductor nanomaterials can often display unique optical, electronic, and magnetic properties, whereas these properties strongly depend on the size and shape of the nanoparticles [1]. As a result, synthetic control over the morphology, size, and crystallographic orientation of materials is highly desired [2]. Among the methods for the preparation of nanomaterials, growing of inorganic structures directly on an organic template has recently emerged as a powerful technique [3]. Perylenetetracarboxylic diimide (PDI) derivatives have been extensively and intensively investigated as advanced molecular materials [4]. In particular, because of their great potential application as organic semiconductors in different molecular electronic devices, the fabrication of ordered nanostructures of these functional molecular materials has become an attracting research area in the past decade [5]. The semiconducting PDI-based organic/inorganic composites in nanoscale should be highly desired for nano-optoelectronic materials due to the possibility of combining desired properties from both. In the present paper, we reported controlled preparation of ZnS nanoparticles in a self-assembled (SA) film of amphiphilic PDI derivative modified with distinctly different hydrophobic/hydrophilic side-chains, N-hexane-N'-(1-phenyl-4-aminoethanol)-1,7-di(4-tert-butylphenoxy)perylene-3,4;9,10-tetracarboxylate diimide (HH-PDI), Fig. 1. By using SA film of amphiphilic HH-PDI molecules as a template, the monodisperse HH-PDI/ZnS nanocomposites were prepared at the air–water interface. The enhanced semiconducting properties were observed for the hybrid nanocomposites relative to respective the pure HH-PDI film.

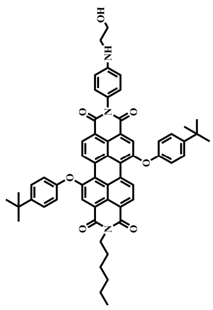

Fig. 1 The molecular structure of HH-PDI.

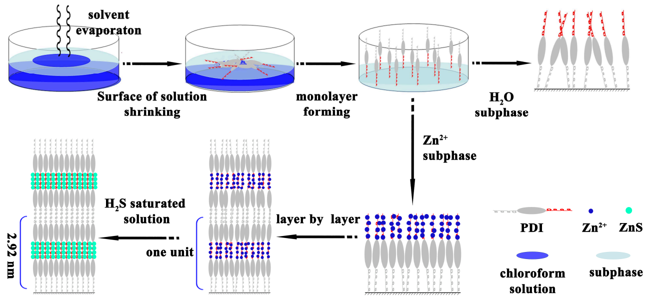

Fig. 2 Procedures for the fabrication of the HH-PDI and HH-PDI/ZnS nanocomposites.

Experimental Section

Chemicals

The sample of HH-PDI was synthesized according to previously published procedures [6]. All the chemicals are analytical reagents and used without further purification.

Preparation and characterization of the HH-PDI SA film and HH-PDI/ZnS nanocomposites

(Fig.2)**.** Prior to the deposition, substrates were successively sonicated in dichloromethane, methanol and distilled water and dried with argon gas. (i) HH-PDI (HH-PDI/Zn^{2+}) SA film: 5.0 mL of dichloroform solution (0.20 mg mL^{-1}) was put into a culture dish (diameter: 9 cm, height: 1.8 cm), then 50 mL water (or ZnSO$_4$ aqueous solution 0.081 mg mL^{-1}) was slowly added onto the surface of the solution. (caution: the amount of water added cannot cover completely the air/CH$_2$Cl$_2$ interface so as to keep the path for the evaporation of CH$_2$Cl$_2$ solvent). During solvent evaporation, HH-PDI molecules gradually assembled to form some fine nanostructures at the CH$_2$Cl$_2$-water interface. After complete evaporation of CH$_2$Cl$_2$, the densely packed film remained on the water surface. Then, the film can be easily transferred from the water surface onto a quartz or Si/SiO$_2$ substrate by horizontal lifting. This process was repeated to obtain the required number of layers. Residual water on the substrates, between transfer steps and after the final transfer, was removed with a stream of nitrogen. (ii) HH-PDI/ZnS nanocomposites: HH-PDI/Zn^{2+} nanocomposites were dipped to a H$_2$S saturated solution (~0.1 mol L^{-1} for 12 h). After being washed with water, the thin film was removed with a stream of nitrogen for SEM (Hitachi S-4300F), X-ray diffraction (Rigaku D/max-γB), UV-vis spectroscopy (Hitachi U-4100) measurements, respectively. The reactions were carried out at room temperature. The device for I-V measurements (Keithley 4200) were fabricated according to previously published procedures [7].

Results and discussion

UV-vis absorption spectra

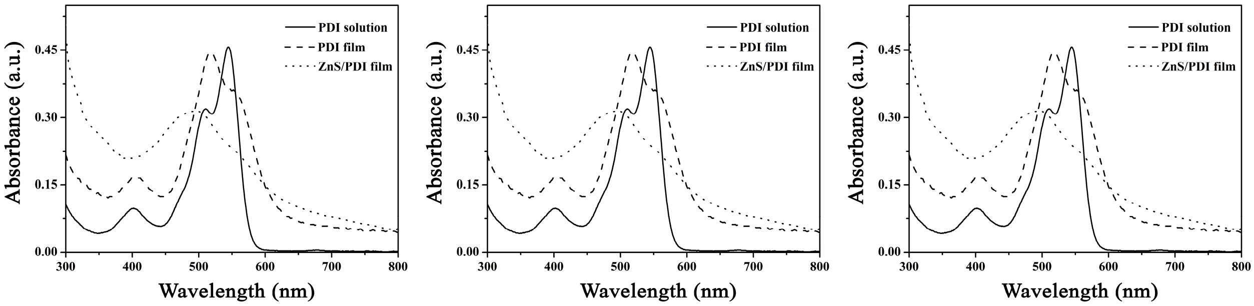

Fig. 3 UV-vis spetra of HH-PDI in dichloroform (solid line) and the HH-PDI pure film (dash line) and HH-PDI/ZnS nanocomposites (dot line). Fig. 4 The X-ray diffraction patterns of HH-PDI pure film (A) and HH-PDI/ZnS nanocomposites (B). The vertical lines show the ZnS powder diffraction pattern from the Joint Committee on Powder Diffraction Standards (JCPDS) Card No. 05-0566.

Fig. 3 displays the UV/Vis spectra of the HH-PDI pure film and HH-PDI/ZnS nanocomposites in comparison with that in the solution. As expected, HH-PDI in dichloroform showed typical feature of the non-aggregated diphenoxy-substituted PDI chromophores in the electronic absorption spectra [8]. The absorptions at about 545 and 514 nm can be attributed to the 0-0 and 0-1 vibronic band of the S_0-S_1 transition, respectively, while the observed absorption band around 402 nm is attributed to the electronic S_0-S_2 transition [6]. Note that the absorption of HH-PDI in the pure film and nanocomposites changed significantly in the ratio of the intensities of the 0-0/0-1 peaks, while peak positions of absorption maxima of HH-PDI remained almost unaltered in the pure film, and blue-shifted to ca.500 nm in the nanocomposites. Those kinds of changes implied the formation of face-to-face π stacks (H-aggregate) and stronger molecular stacking interaction between the PDI skeletons of HH-PDI in the nanocomposites than the pure film [8], which is able to provide the more efficient π stacking and in turn is responsible for the much larger carrier mobilities revealed for the devices fabricated from the former than the latter one(*vide infra*). Furthemore, by comparing the UV-vis spectra of HH-PDI pure film and HH-PDI/ZnS nanocomposites, we can find that the nanocomposites exhibits a higher absorption intensity in the wavelength region below 350 nm, which is very similar to the absorption of bulk ZnS nanoparticles [9], suggesting the ZnS nanostructures have been shaped in the nanocomposites.

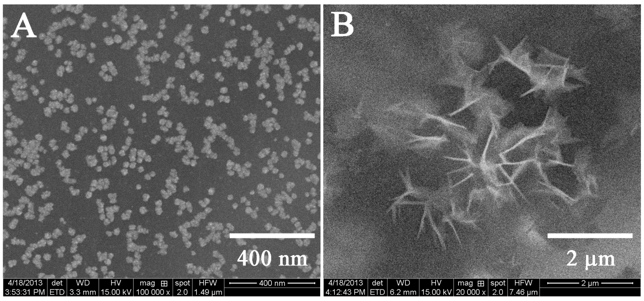

Fig. 5 SEM images of HH-PDI/ZnS nanocomposites (A) and HH-PDI pure film (B).

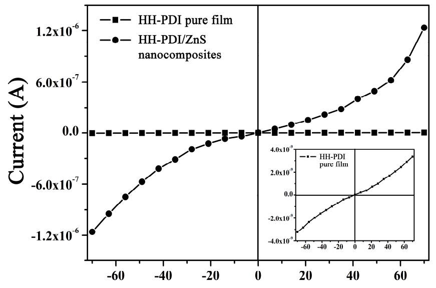

Fig. 6 The current-voltage (I-V) characteristics of the HH-PDI pure film (■), HH-PDI/ZnS nanocomposites (●).

X-ray diffraction (XRD) pattern

The XRD patterns for the HH-PDI pure film and HH-PDI/ZnS nanocomposites are shown in Fig. 4. In the nanocomposites, various diffraction peaks were observed, which were, according to JCPDS file No. 05-0566 (shown as vertical lines in Fig. 4), assigned to the (111), (220) and (311) planes of the cubic phase of zinc blende ZnS. XRD patterns in combination with UV-vis and SEM analysis (*vide infra*) of the samples provided exclusive evidence that ZnS nanoparticles formed exhibit a highly crystalline structure. On the other hand, the XRD pattern of the HH-PDI pure film exhibits the (001) Bragg peak at 2θ = 4.48°, corresponding to a periodic spacing distance of 1.94 nm, Fig. 4A. Consequently, orientation angle of HH-PDI rings with respect to the substrate surface of ca. 59.4° are estimated for HH-PDI in pure film based on the length of HH-PDI (2.30 nm) taken from the energy-optimized structure. A slipped co-facial stacking mode with the molecular long-axis perpendicular to the substrate surface (H aggregate) was achieved for HH-PDI [10], which is in line with that UV-vis absorption. In addition, the appearance of a broad peak at 0.42 nm for the HH-PDI pure film suggested that there exists liquid-like ordered packing of long alkyl chains [6]. A sharper peak at 0.31 nm (2θ = 28.9°) obtained for the HH-PDI pure film is ascribed to π-π stacking distance of PDI rings between the adjacent molecule, implied a favorable molecular packing from co-facial conformation depending mainly on the π-π interaction between perylene rings in the HH-PDI film. However, in the HH-PDI/ZnS nanocomposites, as shown in Fig. 4B, the XRD diagram shows two well-defined low-angle diffraction peaks at 2θ = 3.01° and 6.07° (corresponding to a periodic spacing distance of 2.92 and 1.46 nm), which are ascribed to the diffractions from the (001) and (002) planes of HH-PDI, indicating the long range molecular ordering across the thickness of the nanocomposites. Due to the special asymmetric molecular structure of HH-PDI, the value of *d* (2.92 nm) in the nanocomposites is actually the thickness of the bilayer (Fig.2). Meanwhile, the diffraction at 0.42 nm disappeared, indicating that the long hydrophobic alkyl chain of HH-PDI in the nanocomposites might no longer take an extended conformation but a folded and tangled conformation instead. Consequently, a significant decreased monolayer thickness (1.46 nm) of HH-PDI obtained in the nanocomposites as compared to that in the HH-PDI pure film can be achieved. Therefore, ZnS crystals grown on HH-PDI organic template has a remarkable influence on the assemble structure of both hydrophobic and hydrophilic side-chains attached to HH-PDI in the nanocomposites.

Morphology of the HH-PDI pure film and HH-PDI/ZnS nanocomposites

As revealed by the scanning electron microscope (SEM), Fig. 5A, the unique nanoparticles were obtained with the average diameter of ca. 20 nm for HH-PDI/ZnS nanocomposites. This is in good contrast to the sheet-like microstructure with large gaps and cracks between aggregate domains observed for HH-PDI molecules in pure film, Fig. 5B, which will surely add negative effect on the electronic conductivity for the I-V devices fabricated.

Semiconducting properties

Fig. 6 shows the current-voltage (I-V) characteristics of the HH-PDI pure film and HH-PDI/ZnS nanocomposites. According to the equation reported in the literatures [7], the electronic conductivity, is calculated to be around 6.6×10^{-5} and 3.6×10^{-7} S cm^{-1} for the HH-PDI pure film and HH-PDI/ZnS nanocomposites, respectively. Comparing with the HH-PDI pure film, the improved conductivity for the nanocomposites might be attributed to readily π- stacks with adjacent planar molecules and the introduction of ZnS n-type semiconducting nanocrystal. The absence of traps or defects in these nanocomposites with more efficient π-π stacks should favour charge transport.

Summary

The well-defined HH-PDI/ZnS hybrid nanoparticles have been successfully prepared at the air-water interface by using SA film of amphiphilic HH-PDI molecules as a template. The significantly improved semiconducting properties are achieved for the resulting nanocomposites. The present result represents the first effort towards controlling the size and morphology of ZnS nanostructures via an amphiphilic asymmetric PDI derivate, which is helpful towards designing, preparing new nanomaterials and more complex nanostructures with tunable functionality.

Acknowledgment

Financial support from the Natural Science Foundation of China (21371073) and the Natural Science Foundation of Shandong Province (ZR2011BZ005) is gratefully acknowledged.

References

[1] J. H. Zhan, X. G. Yang, D. W. Wang, S. D. Li, Y. Xie, Y. Xia, Y. Qian, Polymer-Controlled Growth of CdS Nanowires, Adv. Mater. 12, (2000), 1348-1351.

[2] C. C. Chen, J. J. Lin, Controlled Growth of Cubic Cadmium Sulfide Nanoparticles Using Patterned Self-Assembled Monolayers as a Template, Adv. Mater. 13, (2001), 136-139.

[3] Y. Lu, Y. Yang, A. Sellinger, M. Lu, J. Huang, H. Fan, R. Haddad, G. Lopez, A. R. Burns, D. Y. Sasaki, J. Shelnutt, C. J. Brinker, Self-assembly of Mesoscopically Ordered Chromatic Polydiacetylene/Silica Nanocomposites, Nature 410, (2001), 913-917.

[4] F. Würthner, Perylene Bisimide Dyes as Versatile Building Blocks for Functional Supramolecular Architectures, Chem.Commun. 14, (2004), 1564-1579.

[5] J. Locklin, D. Li, S. C. B. Mannsfeld, E. J. Borkent, H. Meng, R. Advincula, Z. Bao, Organic Thin Film Transistors Based on Cyclohexyl-Substituted Organic Semiconductors, Chem. Mater. 17, (2005), 3366-3374.

[6] H. Wu, L. Xue, Y. Shi, Y. Chen, X. Li, Organogels Based on J- and H-Type Aggregates of Amphiphilic Perylenetetracarboxylic Diimides, Langmuir 27, (2011), 3074-3082.

[7] Y. Chen, M. Bouvet, T. Sizun, Y. Gao, C. Plassard, E. Lesniewska, J. Jiang, Facile approaches to build ordered amphiphilic tris(phthalocyaninato) europium triple-decker complex thin films and their comparative performances in ozone sensing, Phys. Chem. Chem. Phys. 12, (2010), 12851-12861.

[8] A. You, J. Gao, D. Li, M.l Bouvet, Y. Chen, Effects of metal–ligand coordination on the self-assembly behaviour of a crown ether functionalised perylenetetracarboxylic diimide, Supramolecular Chemistry 24, (2012), 851–858.

[9] A. Takeo, S. Shin-ichiro, S. Yoshinori, T. Hideyuki, S. Kozo, J. Balachandran, T. Kazuyuki, Cu-Doped ZnS Hollow Particle with High Activity for Hydrogen Generation from Alkaline Sulfide Solution under Visible Light, Chem. Mater. 20, (2008), 1997-2000.

[10] M. Kasha, H. R. Rawls, M. A. E. Bayoumi, The Excition Model in Molecular Spectroscopy, Pure Appl. Chem. 11, (1965), 371-392.

Materials Science and Engineering Technology

10.4028/www.scientific.net/AMR.936

A Facile Method to Preparation of Amphiphilic Perylene Tetracarboxylic Diimide/ZnS Hybrid Nanocomposites and Improved Semiconducting Property

10.4028/www.scientific.net/AMR.936.295